Effect of the isotope mass on the turbulent transport at the edge of L-mode plasmas in ASDEX Upgrade and JET-ILW

N. Bonanomi[1], C. Angioni[1], P. C. Crandall[1,3], A. Di Siena[1], C. F. Maggi[2], P. A. Schneider[1], the ASDEX Upgrade Team, the EUROFusion MST1 Team* and JET Contributors**

1) Max Planck Institute for Plasma Physics, Boltzmannstr. 2, 85748 Garching, Germany
2) Culham Centre for Fusion Energy, Abingdon, OX14 3DB, UK
3) University of California, Los Angeles, USA
*See the author list H. Meyer et al 2017 Nucl. Fusion 57 102014
**See the author list of "Overview of the JET preparation for Deuterium-Tritium Operation" by E. Joffrin et al. to be published in Nuclear Fusion Special issue: overview and summary reports from the 27th Fusion Energy Conference (Ahmedabad, India, 22-27 October 2018)

Since the first comparisons between different hydrogen isotope plasmas in tokamaks it appeared that deuterium (D) plasmas have a better performance than hydrogen (H) plasmas [1-3]. These experimental observations are in opposition to early theoretical predictions that indicate a gyro-Bohm mass scaling for the turbulent transport ($\chi_i \propto m_{isotope}$, e.g. Ref. [4]), this contrast between theory and experiment generally referred to as 'isotope effect'. A general experimental observation is that the effects of the isotope mass in the plasma edge of L-modes and in the plasma pedestal of H-modes play an important role. The L-H power threshold and the H-mode pedestal [1,3,5,6] have been found to depend on the ion isotope mass. Understanding how the isotope ion mass is acting on these parameters is then essential for predicting future reactors such as ITER (International Thermonuclear Experimental Reactor). We focus our study on the nature of the turbulent transport in ASDEX Upgrade and JET-ILW (Joint European Torus with the ITER-Like Wall) L-modes edge focusing on the effect of the isotope mass on the turbulence. We use gyrokinetic simulations with experimental input parameters and compare the results with the available experimental measurements. Thereby, we can study and compare the nature of the turbulent flux in experimental relevant conditions in different machines.

The experimental data are taken from the ASDEX Upgrade tokamak (AUG, R_0=1.65 m, a = 0.55 m) with a full tungsten wall and from the JET tokamak (R_0=2.96 m, a=1 m) with the ITER-Like Wall (ILW, tungsten divertor and beryllium main chamber). For both devices a pair of H and D discharges with same toroidal field (B_T=2.5 T for AUG and B_T = 3.0 T for JET), plasma current (I_p=0.8 MA for AUG and I_p=2.5 MA for JET), plasma shape and matched temperature and density profiles (see Fig.1) have been considered.
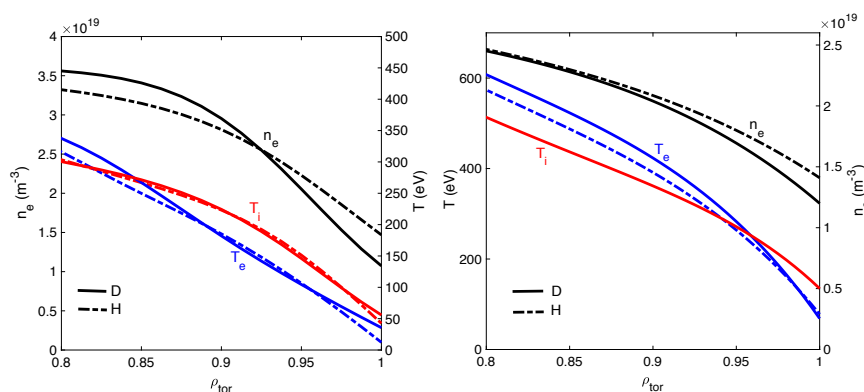

Fig.1) Fits of the density (n_e) and of the temperatures (T_e, T_i) profiles for the AUG (a) and JET (b) H and D discharges.

In order to obtain similar profiles, more heating power (~ 30% in AUG and ~ 40% in JET) and more gas puff (0-30% in AUG and ~ 30% in JET) were necessary in the H discharges. ECRH (Electron Cyclotron Resonance Heating) heating was used in AUG (0.5 MW in D and 0.81 MW in H), while NBI (Neutral Beam Injection) heating was used in JET (3.4 MW in D and 4.5 MW in H). More information on the experimental

settings and methods used for analysing these discharges can be found in Ref. [3,7]. While in both cases n_e, T_e and T_i are almost matched, as well as the values of $R/L_{Ti,e} = -R \cdot \nabla T_{i,e}/T_{i,e}$, the values of $R/L_n = -R \cdot \nabla n/n$ are lower in the H plasmas, especially in AUG. This difference in the edge density peaking between H and D plasmas has been already observed in the past in ASDEX Upgrade and could play a role in the different L-H threshold between H and D plasmas.

Using the experimental parameters as input, linear and non-linear gyrokinetic simulations with the GENE (Gyrokinetic Electromagnetic Numerical Experiment) code [8] have been performed at $\rho_{tor} = 0.925$ for the AUG discharges and at $\rho_{tor} = 0.95$ for the JET discharges ($\rho_{tor} = \Phi/\Phi^{max}$, Φ being the toroidal magnetic flux). The simulations are carried out using realistic geometry, collisions, finite-β effects (considering $B_\perp$ and $B_{//}$ fluctuations), kinetic ions and electrons (no impurities are considered as Zeff~1.2). Typical grid parameters in the non-linear simulations are as follows: perpendicular box sizes $[L_x, L_y]$~$[500,250] \rho_s$, phase-space grid $[n_x,n_y,n_z,n_{v//},n_\mu]$~$[512,70,70,32,16]$ and k_y^{min}~0.02 (z is the coordinate along the magnetic field line, x is the radial coordinate, y is the binormal coordinate, $v_{//}$ is the parallel velocity, μ is the magnetic momentum and $\rho_s = (m_i T_e)^{0.5}/eB_{ref}$). All the simulations have been done in the local limit except few linear global simulations. The use of periodic boundary conditions in local simulations had to deal with the appearance of radially elongated structures of the parallel magnetic potential $A_{//}$ that could not be resolved with a radial box size $L_x < 400 \rho_s$, while the electrostatic potential ϕ structures could be resolved also with narrower box (L_x~$120 \rho_s$). It is worth noticing that the heat fluxes were not affected by the
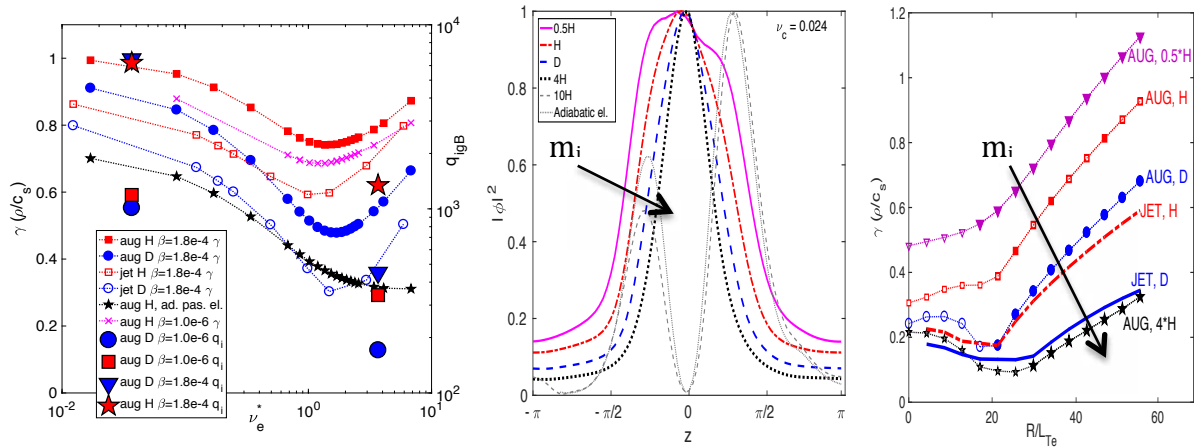

Fig.2) Linear growth rate γ (ρ_s/c_s) and non-linear q_i (kW/m^2) v/s ν_e^* (left). $\Phi(z)$ structures with different isotope mass (center). γ (ρ_s/c_s) v/s R/L$_{Te}$ with different isotope mass (right).

size of L_x once the structures of ϕ were well resolved. In order to have stable results even at very high level of collisionality, the 'Landau-Boltzmann' operator in GENE has been used. For more details see Ref. [9].

The linear gyrokinetic simulations indicate that drift-wave instabilities with negative frequency ω are dominant in the considered cases. The drift-wave nature of the instability appears from the phase-shift angle (α) between ϕ and T_e fluctuations, being $\alpha < \pi/2$, and from the ballooning structures of ϕ and $A_{//}$, ϕ having a ballooned structure with tails and $A_{//}$ structures being asymmetric with a minimum at $\theta = 0$. A scan in the normalized collision frequency $\nu_e^* = 4/3\pi^{0.5} \nu_{ei} qR^2/\varepsilon^{1.5}/v_{th,e}$, where $\varepsilon = r/R$ and $v_{th,e} = (T_e/m_e)^{0.5}$, at $k_y \rho_s = 0.2$, is shown in Fig. 2. Collisions are stabilizing at first but, beyond a certain value corresponding to a minimum in the linear growth rate γ (ρ_s/c_s), they have a destabilizing effect. The

experimental range of parameters of the studied discharges lies in the region close to the minimum in γ where collisions are destabilizing. The dynamics of passing kinetic electrons is fundamental for the instability at high collisionality: when adiabatic passing electrons are considered, collisions have a stabilizing effect also at high values of ν_c (see Fig.2). Looking at the contribution to the growth rate of the electron curvature term, that is the main linear drive of the instability, it also appears that, when increasing collisionality, the region in the velocity space that contributes to γ changes from being strongly dominated by the trapped particle region (as expected for trapped electron modes) to a strong contribution from the passing particle region. Also the effect of the isotope mass depends on ν_c. The different isotope ion mass appears to influence the parallel structure of the electrostatic potential $\phi(z)$, as shown in Fig.2. The structure of $\phi(z)$ is broader for lower isotope mass, this behaviour being strongly enhanced at high collisionality and not related to a change in the effective collisionality due to a change of the ion mass. This suggests a role of m_e/m_i when the electron parallel dynamics is strongly damped by collisions. The effect of the ion mass at high collisionality translates into a different threshold in R/L_{Te} with different isotope mass (Fig.3). The effect of R/L_n on these modes has a non-monotonic behaviour while no strong dependence on R/L_{Ti} has been observed in the linear simulations.
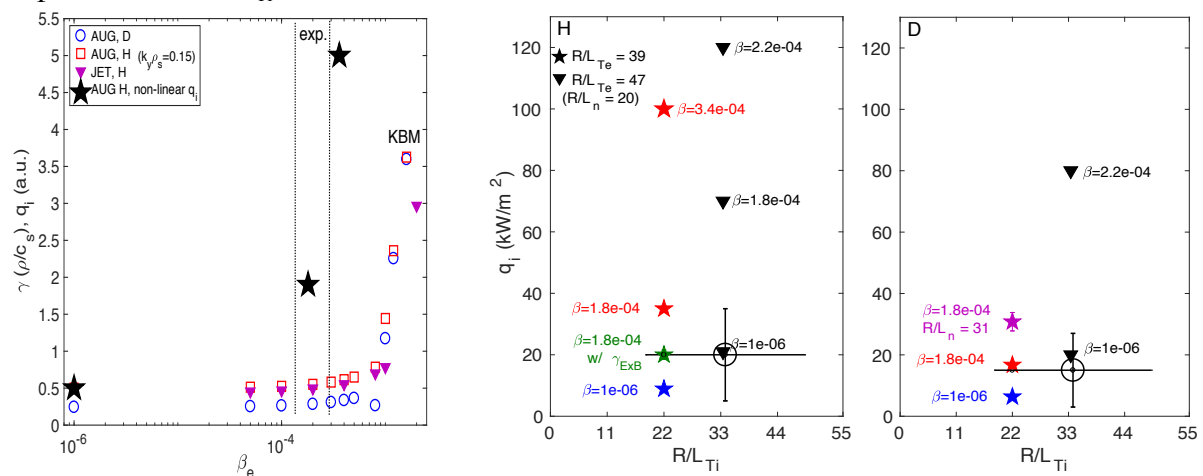

Fig.3) Linear growth rate γ (ρ_s/c_s) and non-linear AUG q_i (a.u.) v/s β_e (left). AUG q_i (kW/m^2) v/s R/L_{Ti} for H (center) and D (right). Similar results have been obtained for JET.

The non-linear simulations confirm some of the results found linearly. The nonlinear saturated state is dominated by electron-drift-wave turbulence with frequencies and phase-shifts similar to those obtained in the linear simulations for $k_y\varrho_s>0.15$. The simulations predict higher fluxes in H with respect to D (see Fig.2 and Fig.3), following the trend found linearly for the growth rate. In contrast to what observed in the linear simulations, electromagnetic effects are fundamental in the non-linear simulations and the non-linear fluxes are very sensitive to β_e (see Fig.2 and Fig.3). The fluxes predicted by the electrostatic simulation are, for both JET-ILW and ASDEX-Upgrade, comparable with the experimental values. When electromagnetic effects are included in the simulations, a strong enhancement of the fluxes is observed and the values of β_e and/or R/L_{Te} must be lowered (within error-bars) in order to match again the experiment. In the electromagnetic simulations there is a strong enhancement of the contribution to the turbulent flux from the low-k_y wave-numbers, with a shift of the peak of the flux spectra to lower k_y. Furthermore, for the same parameters, the enhancement of the fluxes is stronger in the H cases. This can be related to the fact that, for the same value β_e, in the linear simulations the drift-wave instability has a lower threshold in H than in D, especially at low k_y. It is important to notice that the fluxes are, also in the electromagnetic

simulations, determined by the electrostatic potential. Regarding the effect of the different R/L_n between D and H, when the higher R/L_n is used in D simulations, the fluxes increase for AUG, reaching the level of the H fluxes. Finally, as visible in Fig.3, when considering the external flow shear, γ_{ExB}, in the H simulations, the heat flux is reduced, indicating that the edge turbulence is affected by the external flow shear even if the value of γ_{ExB} is low (but comparable with $\gamma(\varrho_s/c_s)$ at $k_y\rho_s\sim0.15$, where the heat flux spectra peaks).

To conclude, the nature of the turbulent transport in the edge of ASDEX Upgrade and JET-ILW L-modes has been investigated through linear and local non-linear gyrokinetic simulations. For both devices the turbulence is found to be dominated by an electron drift-wave destabilized by the high collisionality in the plasma edge and strongly related to the kinetic electron dynamics. This result, which is obtained here with specific parameters of ASDEX Upgrade and JET-ILW plasmas, confirms past general edge turbulence studies and simulations [10-12]. The turbulence in the edge is found to be strongly influenced by electromagnetic effects, with a strong enhancement of the contribution to the turbulent fluxes from low k_y wave-numbers observed when electromagnetic effects are included. This strong effect is not observed in linear simulations below the kinetic ballooning modes (KBM) threshold. Regarding the effect of the isotope mass, the main linear instability is found to be more unstable with lighter isotope mass at high collision frequency. This effect is related to broader eigen-functions of $\phi(z)$ and translates into a lower linear threshold in R/L_{Te}. This effect takes place only at high value of collisionality, while, at levels typical of the plasma core, this effect is negligible. This result supports the role of the collisionality in damping the parallel electron dynamics allowing the ion mass to have a stronger effect on the instability. The non-linear simulations confirm that the turbulence is stronger with lower isotope mass, with higher particle and heat fluxes with lower isotope mass in both the electrostatic and the electromagnetic simulations. The combination of higher heat and particle transport in H plasmas, limiting temperature and density gradients, also lead to the requirement of a higher separatrix density to reach the same line averaged density, in agreement with the experimental observations. This can indeed contribute to determine the higher L-H power threshold in H plasmas with respect to D plasmas. Also, the turbulent fluxes have been found to be sensitive to the external ExB flow shear, even for the low experimental level of γ_{ExB}, supporting the hypothesis of a role of the γ_{ExB} driven by the radial electric field in suppressing the edge turbulence helping the formation of the external transport barrier and the L-H transition. These results are also in agreement with the hypothesis, already expressed for the JET-ILW cases in Ref. [3], that the turbulent transport plays a determinant role in explaining the different plasma edge behaviour and the higher L-H power thresholds with different isotope masses. Remarkably, when considering all the effects in the non-linear simulations, the predicted fluxes can reproduce the experimental fluxes and the experimental behaviour with the isotope mass.

References
[1] M. Bessenrodt-Weberpals et al., Nucl. Fusion 33 (1993).
[2] C.W. Barnes et al., Phys. Plasmas 3 (1996).
[3] C. F. Maggi et al., Plasma Phys. Control. Fusion 60, (2018).
[4] G. Manfredi et al. Phys. Rev. Lett. 79 (1997).
[5] F. Ryter et al., Nucl. Fusion 49, 062003 (2009).
[6] E. Righi et al., Nucl. Fusion 39, 309 (1999).
[7] P. A. Schneider et al., Nucl. Fusion 57 (2017).
[8] Jenko F. et al., Phys. Plasmas 7, 1904 (2000).
[9] N. Bonanomi et al., subm. to Nucl. Fus. 2019.
[10] B.D. Scott, Plasma Phys. Control. Fusion 49, S25 (2007).
[11] B.D. Scott, Phys. Plasmas 12, (2005).
[12] B.D. Scott et al., Contrib. Plasma Phys. 50, No. 3-5, 228 (2010).